Exit Routes from the Transition State: Angular Momentum Constraints on the Formation of Products

Anthony J. McCaffery,*,† Mark A. Osborne,† and Richard J. Marsh‡

Department of Chemistry, University of Sussex, Brighton BN1 9QJ, U.K., and Department of Physics, University College, Gower Street, London WC1E6BT

Received: March 23, 2005

We have analyzed experimental data from a number of exothermic processes in which molecules in well-defined initial states are deactivated by inelastic, dissociative, or reactive collisions. Further, we analyze deactivation processes that do *not* occur in molecules despite their containing high levels of excitation. Significant common elements are found among these forms of deactivation. The initial step consists of transition to a product state involving minimum rotation state change (Δj) consistent with energy conservation. Frequently, this process is near-energy-resonant. More critically, it may frequently require substantial angular momentum (AM) change. Analysis of experimental data indicates that constraints act upon on the formation of products in processes that involve release of excess energy. These constraints are associated with the magnitude of AM that must be generated for the initial transition to occur and this AM "load" increases with the amount of energy to be released. In general, the probability of generating rotational AM falls rapidly as Δj increases, and this effectively limits the size of energy gap that may be bridged by a given reactant pair and at some point the constraint is sufficient to constitute a barrier that prevents the process from taking place. The choice of reactant species strongly affects the probability of each process that increases (i) when molecules efficiently interconvert momentum and (ii) when many product states are available in the critical near-resonant region. These factors increase the proportion of initial trajectories that possess the energy and momentum necessary to open a "product" channel. Evidence is presented showing that AM load-reduction strategies lead to marked enhancement of rates of collision-induced processes, suggesting that reduction of constraints in the exit channels from the transition state may constitute a previously unrecognized form of catalysis.

1. Introduction and Background

The notion that activation precedes reaction is generally attributed to Arrhenius,[1] who first recognized that the marked temperature dependence of reaction rate reported in kinetics experiments[2,3] could not be rationalized in terms of increased kinetic energy of the colliding species. However, equilibrium between "normal" and "activated" molecules introduces an exponential form of temperature dependence through expressions for the fraction of molecules possessing energy in excess of a specified value. As a result, the model of a chemical reaction as a journey from reactant potential well, across an activation barrier and down into the products valley took firm hold. The experimental basis of this notion, though substantial in volume, is quite coarse-grained compared to that obtained using modern reaction dynamics methods. Data refer to reactants equilibrated over vibrational and rotational states with product distributions similarly undiscriminated, and thus the stages by which the system approaches and then departs from the transition state are not resolved.

There have been major advances in the study of the elementary acts of physical and chemical change since this early work, the most detailed being state-to-state studies of inelastic and reactive events under single collision conditions. Here we ask how such experiments advance the concept first proposed by Arrhenius. The primary focus will be on systems that are sufficiently simple for detailed analysis to be performed, though we point out that there are clear indications the conclusions we draw have wider applicability. A number of critical questions are of relevance, for example:

1. What can inelastic and dissociative processes tell us about reactive encounters?

2. What product quantum channels dominate the post-collision distribution and what relation do they bear to the initial state?

3. What can be learned from processes that do *not* occur?

Much reaction dynamics research has focused on how best to activate molecules in *entrance* channels to the transition state through, e.g., optimizing steric factors or by selective use of translational, vibrational, or rotational excitation.[4] In studies of the kinetics and dynamics of bimolecular reactions, little consideration appears to have been given to the possibility that the *products* side of the reaction profile might offer opportunities for enhancing the overall reaction efficiency. The assumption, embodied in the quasi-equilibrium hypothesis of transition state theory, is that products are rapidly removed from the reactants ↔ products equilibrium and play little part in the overall probability of reaction. However, state-to-state experiments make clear that nascent products are formed in excited rovibrational states[5] and subsequently are deactivated by events presumed similar in kind to those that form the activated complex from reactants. Thus consideration should at least be given to the possibility that post-transition state energy and momentum disposal might influence the rate at which a reaction occurs or indeed whether a reaction can proceed to products.

* Corresponding author. E-mail: a.j.mccaffery@sussex.ac.uk.
† University of Sussex.
‡ University College.

10.1021/jp051509p CCC: $30.25
Published on Web 05/19/2005

The purpose of this article is to describe experimental evidence that the manner by which an activated molecule disposes of its excess energy strongly influences (i) the probability that the process occurs at all and, (ii) if the process does occur, the factors that govern the rate constant for the reaction. The evidence indicates that there are constraints acting upon the formation of products and these constraints will always be present when an excited molecule must dispose of relatively large amounts of energy under conditions imposed by the conservation laws. We demonstrate this to be a general property that affects deactivation of species in inelastic, dissociative, and reactive events. An understanding of the factors that govern efficient energy and momentum disposal in exit channels allows guidelines to be proposed for enhancing reaction rates based on the properties of the products. Furthermore, the well-known resistance of certain highly excited species to relaxation allows certain product species to be identified and classed as potentially undesirable because with these, the prospect of reverse reaction will be enhanced.

In sections 2 and 3 below we describe state-to-state, single collision, experimental data in which activated molecules are deactivated by inelastic collision or by dissociation. Each is accompanied by the release of energy and the analogy to exothermic chemical reactions is developed. Three distinct forms of molecular transformation are considered and in each case data from state-to-state molecular dynamics experiments are available. We begin with examples of vibrational relaxation in di- and polyatomic species and consider why deactivation takes place in some instances whereas in others the process does not occur. We next consider vibrational predissociation (VP) of a series of van der Waals (vdW) complexes in which excitation of a vibrational mode in the chemically bound species leads to breaking of the weak vdW bond and subsequent vibrational deactivation. The third category consists of a number of elementary chemical reactions where analogies to energy disposal in the inelastic and dissociative cases are developed in more detail. The analysis utilizes the angular momentum (AM) model that we have developed in recent years.[6−8] Formulation of this model followed analysis of results from collision dynamics experiments that indicate the driving force in elementary processes of physical and chemical to be *momentum* change. Quantization and energy conservation are added to a process in which the motive force is Newtonian and thus directly related to change of momentum (dp/dt), in particular its conversion into molecular rotation.

The AM method is a simple and visual form of mechanics, the parameters of which are related to familiar quantities such as molecular shape, size, and mass. Velocity−angular momentum plots give qualitative indication of the likely outcome of a collision-induced transition, and these yield considerable insight into the physical factors that determine these outcomes.[6−8] Quantitative calculations are based on a 3-dimensional, hard ellipsoid representation having ($a - b$) = half bond length (HBL) of a (homonuclear) diatomic molecule where a and b are respectively semimajor and semiminor ellipse axes. This shape is found to give an accurate form of the key probability density $P(b_n)$ in calculations.[6] The transparency of the principles upon which the AM model is based allows molecules to be categorized according to an efficiency factor[6−8] that quantifies the ability of a species to dispose of excess energy as molecular rotation. This appears to be a key process in energy-releasing inelastic and dissociative events. Angular momentum conservation often will require the excitation of product molecules to high rotational levels, and this emerges as a controlling factor in inelastic, dissociative, and reactive events. A number of di- and polyatomic molecules generate molecular rotation from an impulse very efficiently whereas others are inefficient. A third category, exemplified by the heteronuclear diatomic hydrides, display eccentric collisional behavior and this often results in very inefficient deactivation of such species, especially when they are highly excited.[7,8] The manner in which the efficiency of momentum conversion influences the probability of reaction is developed in the following sections.

2. Energy Release in Inelastic and Dissociative Events

2.1. Deactivation of Vibrationally Excited Molecules by Inelastic Collisions. In any collision-induced processes the interaction causes the molecule to undergo transition from its initial quantum state, with well-defined electronic, vibrational, and rotational quantum numbers, to a new state in which one or more of these quantum numbers has changed. Vibrational deactivation is analogous to the post-transition state events of an exothermic chemical reaction in that energy is released into "products". It differs of course in that these "products" are "reactants" that have undergone no more than a quantum state change. However, the simplicity of the process allows very detailed analysis of factors controlling the deactivation. Vibrational energy is converted into molecular rotation and relative motion of the collision pair. When the partner is an atomic species, the analysis may be very precise. Several state-to-state studies have been published the most detailed of which consist of extensive rate constants for vibration−rotation transfer (VRT) in $(A)^1\Sigma_u^+Li_2-X$ (X = rare gas).[9] In these experiments the diatomic is initially excited to a very precisely defined, high-lying rovibrational level of the excited (A) state and spectrally resolved fluorescence allows rate constants for individual state-to-state transitions to be determined.

The amount of excess energy initially contained within the Li_2 molecule is considerable, being of the order of 2 eV. This high level of excitation in a molecule of relatively low vibrational energy ($\omega_e = 255.47\ cm^{-1}$) means that unusually large Δv processes occur and vibrational change up to $\Delta v = -5$ has been reported in the case of Li_2^*-Xe collisions from (v_i, j_i) = (9, 42).[9] Collision-induced transitions were detected and rotational state distributions measured for $v_f = 4-12$. Two aspects of these data are of significance: (i) The peak of the rotational distribution shifts markedly with Δv. The highest intensity Δj transition represents the most favored exit channel for the relaxation, i.e., optimizing the disposal of available energy. (ii) Transitions with $\Delta v > -5$ are *not* seen. This is surprising because the (9, 42) → (0, Δj) transition would release more energy than the $\Delta v = -1$ to -5 processes that *are* observed.[10] The general expectation is that activated molecules, i.e., those possessing excess energy, tend to lose the excess and return to the lowest level as rapidly as possible. When this does not occur, or when a system with a large surplus of energy deactivates more slowly than one with a small excess, we look for the presence of "selection" or "propensity" rules that moderate the transition probability if all other factors are equal. Here it appears that constraints on energy release rapidly increase with Δv up to a certain point beyond which the transition probability has effectively fallen to zero.

We consider initially the first of these issues, namely the most favored exit channels, to identify features of a collision-induced transition that are positively enhancing and focus primarily on the exothermic process $\Delta v = -3$. Figure 1a is an energy level diagram showing the initial (9, 42) state and rotational levels of $v = 6$ and $v = 0$. Arrows from (9, 42) indicate the principal

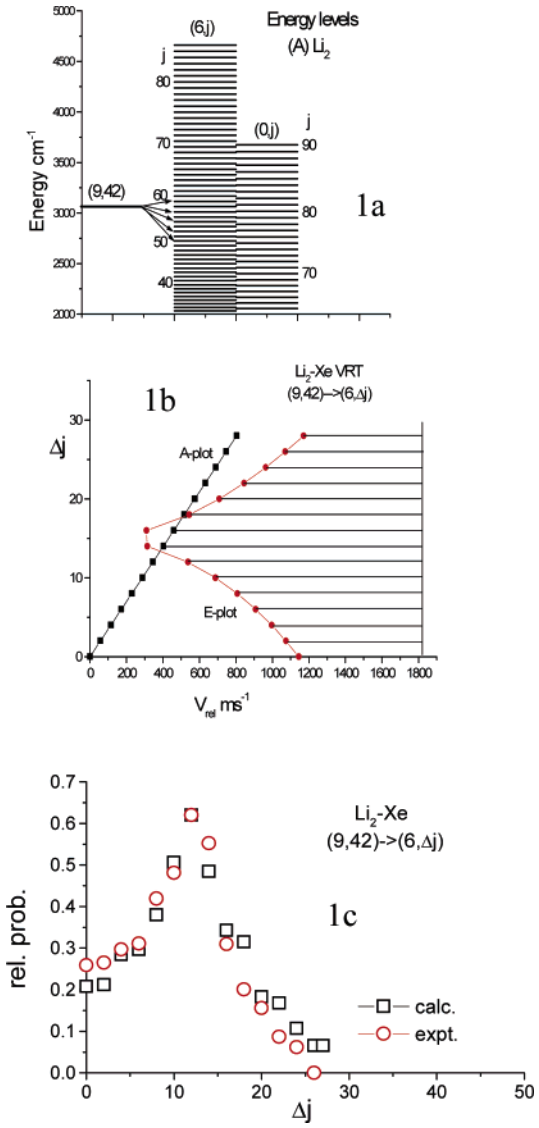

Figure 1. (a) Energy level diagram showing initial (9, 42) and final (v_f, j_f) levels of (A)$^1\Sigma$ Li_2 for $v_f = 6$ and 0. Arrows denote principal observed collision-induced transitions. (b) Velocity−angular momentum diagram showing channel-opening threshold velocities for transitions (9, 42) → (6, Δj) allowed by energy conservation (*E* plot) and AM conservation (*A* plot). (c) Experimental (red circles) and calculated (black squares) Δj distribution for (9, 42) → (6, Δj). Note that in (b) and (c), Δj is plotted from $j_i = 42$. Experimental data taken from ref 9.

collision-induced $\Delta v = -3$ transitions, found[9] experimentally to peak at $\Delta j = 12$ ($j_f = 54$) of $v = 6$. Thus the most favored exit transition involves generation of 12 additional units of rotational angular momentum in Li_2. The reason this channel is favored is apparent from Figure 1b, a velocity−angular momentum plot for the transitions (9, 42) → (6, Δj). These plots were introduced[11] as a means of illustrating the constraints imposed on collision-induced transitions by angular momentum conservation and by energy conservation in the AM theory of collisional transfer and have been widely used in the analysis of VRT and other processes.[8] The shaded region of Figure 1b indicates those relative velocities fully allowed by energy and AM conservation that can contribute to the individual Δj channels shown. Low-Δj processes are strongly constrained by energy conservation requirements and this causes severe restrictions on possible values of b_n, the effective impact parameter in the conversion of linear-to-angular momentum (expressed as $\Delta j = \mu v_r b_n$),[6−8] and on the range of v_{rel} values that may contribute to these channels. These restrictions are removed for $\Delta j = 14$ (and 16) and the rotational distribution peak in vibrational relaxation generally occurs at or close to the minimum Δj for which energy conservation restrictions have been lifted. This approach allows accurate prediction of the rotational peaks for all other Δv processes in Li_2*−Xe and for a wide range of other collision systems.[8] Quantitative calculations based on these principles accurately reproduce experimental data as Figure 1c demonstrates for (9, 42) → (6, Δj) VRT in Li_2*−Xe.

The experimental data and above analysis indicate that the initial step in energy release from Li_2* involves transitions that are near-energy-resonant with the initial state in a process in which vibrational energy is converted into molecular rotation. *The distribution peak is generally at (or just below) the lowest Δj value for which the energy conservation condition allows the greatest number of velocities, and hence trajectories, to contribute. Alternatively, it is the lowest Δj channel for which AM is the dominant constraint when b_n^{max} is the maximum value available in the system concerned.* The rotational AM change required for the most favored transition increases as Δv increases and is $\Delta j = 4$, 8, 12, 16, 20 for $\Delta v = -1$, −2, −3, −4, −5, respectively. In each case the peak corresponds to the first crossover point of the angular momentum and energy conservation relations (*A*- and *E*-plots respectively) and the value of Δj required for this process could be thought of as the rotational AM "load" that must be overcome for this most favored transition to occur. The rate constant falls rapidly as Δv increases[9] and reflects the increased difficulty of generating large Δj transitions or, more accurately, the reduced number of trajectories that may access b_n values of sufficient magnitude to create large changes in rotation. Note that in each case more than sufficient energy is available for the transition.

The second issue raised above, namely, why $\Delta v = -9$ does *not* occur (along with $\Delta v = -8$, −7, and probably, −6), appears to be related to the magnitude of the AM load referred to above and the ability of a given collision pair to generate the required amount of AM. The molecule and collision partner both have roles to play because the former determines the maximum torque-arm available and the partner influences the extent of the energetic constraints.[6−8] Thus an analysis similar to that described above predicts that the rotational distribution for $\Delta v = -9$ would peak at $j_f = 84$ and thus require that $\Delta j = 42$. The system would have no difficulty in meeting energy requirements for transitions to $v = 0$ because these transitions would again be near-resonant of the kind shown in Figure 1b and have low channel-opening velocity. However, the transition requires that at least 42 AM units be generated via the mechanism of momentum interconversion. In the absence of specific energy constraints, the probability of a given Δj transition falls in exponential-like fashion as Δj increases.[6,12] *Thus in any collision-induced exothermic event there is a maximum angular momentum that may be generated from a specified molecule−collision partner pair for a given velocity distribution and certain deactivation processes have too low a probability to be observable despite possessing sufficient energy for the transition.* In this instance the AM loads associated with the transitions $\Delta v = -9$, −8, and −7 are too large for transitions even to the most favored rotational levels to have appreciable probability even though the energy threshold in each case is very low.

2.2. Vibrational Deactivation by Cold Collisions. Restrictions on high-Δj transitions noted above in the case of Li_2*−Xe vibrational relaxation might simply reflect the range of relative velocities available in these thermal cell experiments. It may be that the two different sources of energy, i.e., that released in the exothermic event and that from the relative motion of the collision partners, have separate properties. To eliminate this possibility, we next consider the vibrational deactivation of the 6^1 level of S_1 benzene co-expanded in a jet with various collision partners. Here collision energy represents no more than a few percent of that released in the transition from 6^1 to 0^0, the lowest vibrational level of the S_1 electronic state. Early studies of collision-induced vibrational transfer in polyatomic molecules,[13,14] performed in thermal cells and in jets, established that there is a very high degree of selectivity in the pathways for relaxation and these are unrelated to the amount of energy involved in the process. Transitions having large energy gaps were often observed to be more probable than those for which the gap was small. A consistent explanation for this selectivity has yet to emerge.

Rotational states in large molecules are closely spaced and thus state-to-state experiments, routine on diatomics, are difficult to perform. Waclawik and Lawrance[15,16] revealed a significant new element governing the vibrational deactivation of benzene in a study of the dependence of $6^1 \rightarrow 0^0$ transition probability on collision partner. The spectroscopic arrangement of 6^1 and 0^0 states is plotted in Figure 2a in which rotational levels of the destination state are shown. For clarity $k = 0$ levels only are plotted. In the experiment a pulsed laser excites a range of low rotational states of v_6 and the post-collision population of final states is determined from spectrally resolved fluorescence. Rotational distributions were obtained by fitting fluorescence band contours.[15,16] Note that, unlike the case previously discussed where Li_2* was in a high rovibrational state, energy-resonant transitions from 6^1 would involve very large j changes. Waclawik and Lawrance[15,16] report that the $6^1 \rightarrow 0^0$ transition is *not* seen when rare gas atoms are the collision partners but is observed when diatomic and polyatomic partners are introduced, the relative probabilities following the order $H_2 > D_2 > CH_4 > C_2H_2 > N_2$. The extent of 0^0 rotational structure was found to vary strongly with collision partner. More recently, these authors[17] found that the $6^1 \rightarrow 0^0$ transition becomes the dominant relaxation path when the co-expanded species is one that may absorb a large fraction of the 522 cm^{-1} available energy into *vibration*.

An explanation of these observations has recently been given and good fits to experimentally extracted rotational distribution were obtained using an "equivalent rotor" model for collision-induced transitions in polyatomics.[18] Figure 2b represents a momentum−AM plot of the energy and AM threshold conditions for benzene undergoing $6^1 \rightarrow 0^0$ relaxation by H_2 and by Ne. (Note that it is convenient to plot momentum rather than velocity when more than one collision partner interacts with a particular species because the (unmodified) *A*-plot remains constant throughout.) H_2 and Ne are examples of partners that respectively are able and unable to induce the $6^1 \rightarrow 0^0$ relaxation. Alternatively, it might be said that there are constraints that prevent the deactivation transition $6^1 \rightarrow 0^0$ with Ne that are overcome on using H_2 as the collision partner. As we discuss later, H_2 is very effective in this regard but not optimally so. The nature of the constraint is clear from Figure 2b and was described above in the context of limits to deactivation of Li_2* $v = 9$. Experimentally, it is found that the most probable relaxation channel is to the minimum Δj for which AM is the dominant constraint with b_n^{max} the maximum available from that system.[8] From Figure 2b this is predicted to be 22 AM units for Ne (12, 27, and 32 for He, Ar, and Kr, respectively).[18] Experiment[15] indicates that these AM magnitudes are too large to have appreciable probability, though for He there is evidence in the data for a transition of very low intensity.[15]

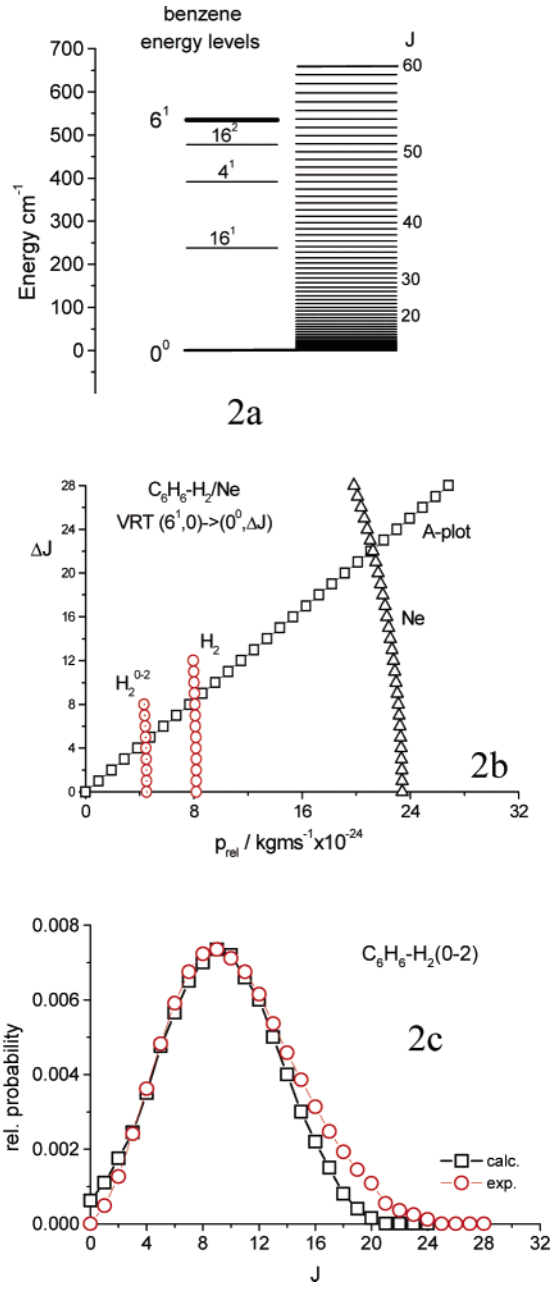

Figure 2. (a) Energy level diagram of some of the low-lying vibrational states of S_1 benzene. The initial 6^1 state is shown together with rotational levels (j changing only) of 0^0. (b) Momentum−AM diagram for the transitions $(6^1, 0) \rightarrow (0^0, \Delta j)$ with Ne and H_2 as collision partners. Plots are shown assuming $0 \rightarrow 2$ rotational excitation in H_2 and with no rotational excitation of H_2. This is seen to have a marked effect on the AM load. (c) Plot of experimental (red circles) and calculated (black squares) rotational distribution in 0^0 assuming $0 \rightarrow 2$ rotational excitation in H_2. The calculated plot represents a weighted sum over a number of j_i states chosen to simulate experimental conditions. Experimental data from Waclawik and Lawrance.[15−17]

Atomic partners have few means of alleviating an AM load in a manner that does not have significant consequences resulting from the generation of increased *orbital* AM. Diatomic partners on the other hand may absorb some of the available energy of

relaxation into rotation or, in favorable cases, vibration and effectively bring about a load reduction. H_2 is particularly useful in this regard, as a small rotational change absorbs a very large amount of energy and, thus, by exciting the $0 \rightarrow 2$ rotational transition in this diatomic, ~70% of the available 522 cm^{-1} $6^1 \rightarrow 0^0$ energy may be shed as partner rotation. The effect of this on the benzene $6^1 \rightarrow 0^0$ rotational AM requirement is shown in Figure 2b. In the absence of partner rotation the predicted most probable exit channel is $\Delta j = 8$, but this reduces to $\Delta j = 4$ on $0 \rightarrow 2$ rotational excitation in H_2—the most probable rotationally inelastic transition in the diatomic. This mechanism provides a plausible explanation for the enhanced intensity of the $6^1 \rightarrow 0^0$ relaxation by H_2. The same transition (or $1 \rightarrow 3$) in D_2 absorbs considerably less of the available energy, and D_2 is predicted to be less efficient than H_2, as are the other collision partners mentioned above.[18] The influence of partner vibrational excitation is discussed in more detail in the next section.

No state-to-state data exist for confirming the mechanism proposed here, and experiments that would fully probe quantum state distributions in each of the participants in a bimolecular collision are still on the horizon. Comparison of rotational distributions extracted from band profiles with those calculated assuming $0 \rightarrow 2$ excitation of H_2 support this interpretation as Figure 2c indicates. Calculations were performed using the equivalent rotor model,[18] an extension of the AM method[6-8] that allows calculation of Δj and Δk cross-sections in polyatomics. Extensive tests of the model on state-to-state data were carried out prior to using the method to calculate VRT probabilities in benzene. Calculations on $6^1 \rightarrow 0^0$ relaxation in benzene were performed for $j_i = 4, 7, 10, 12, 15$ to simulate experimental conditions with scaling factors of 0.8 applied to the $j_i = 10, 12$ data and 0.3 to that from $j_i = 15$. The aggregated results were fitted to a Gaussian distribution and the experimental results normalized to those calculated. As Figure 2c demonstrates, the fit is good. Calculations that do not assume $0 \rightarrow 2$ excitation of H_2 are able to match the observed peak only if $j_i \leq 2$ dominates and the resultant overall fit is poor.

Summarizing this section on exothermic inelastic processes, the principal channel for relaxation of the activated species initially involves the lowest rotational quantum state change to which the greatest number of velocities may contribute. The latter condition results from the energy conservation relation. This channel is also the lowest Δj for which AM is the dominant constraint when the systems maximum available b_n is employed. This principle appears to be independent of the relative contributions to the total energy from kinetic energy of relative motion and that released in the transition. Quantitative AM model calculations agree well with experimental data, indicating the physical principles on which the above analysis is based provide an accurate and reliable representation of the process. The magnitude of the most probable exit channel j-change increases with transition energy gap. Furthermore, the preferred Δj varies with the mass and nature of the collision partner. *For a given collision pair there will be a j-change limit beyond which the transition probability will be too small to detect due to the exponential-like fall of probability with increasing* Δj.

This restriction constitutes a constraint on the deactivation of molecules in activated or excited states, one that affects the available exit channels to "products" from the activated state. The constraint is associated with the (rotational) angular momentum load that must be overcome when energy is released and illustrates the control exerted by momentum interconversion on collision-induced events. Minimum energy pathways are favored when they coincide with low-Δj transitions. These exit channel constraints depend strongly on the nature of the collision pair, and as a general rule it will be advantageous to deposit a sizable fraction of the available energy into collision partner rotation or vibration because this process can greatly enhance the probability of deactivation.

2.3. Vibrational Predissociation of van der Waals Complexes. Molecular photodissociation has been the subject of intensive study for a number of years[19] because, in principle, the exit channel processes may be separated from the collision events that precede reaction. The distribution of dissociation products from species previously excited to a well-defined state probes the exit channel half of the encounter. This "half-collision" event, however, may often be considerably more energetic than a thermal collision and very large amounts of energy indeed may require disposal. An added complexity in photodissociation is that much of this excess energy is in the form of electronic excitation whereas the fundamental events of physical and chemical change, for the most part, consist of exchange of vibrational, rotational, and translational energy. Vibrational predissociation on the other hand is a relatively gentle dissociative event involving low-energy processes and thus is more analogous to a dissociating, chemically activated species.

Weakly bound van der Waals (vdW) species in low-temperature environments are in many respects ideal for the study of dissociation because they may be investigated with great precision and are found to exhibit widely varying lifetimes and rotational distributions on dissociation.[20,21] In a typical experiment a weakly bound molecule−partner pair is formed in a jet expansion and a specific vibrational mode of the chemically bound species is excited. This activation in one part of the molecule eventually causes the weak vdW bond to break and hence the process is closer in kind to a true chemical reaction than an inelastic collision, as now the products differ chemically from the reactants. The observable result of the dissociation, other than the appearance of two independent products, is that the stable species relaxes, with a characteristic time constant, to a lower vibrational level. Combined measurements of rotational distribution and dissociative lifetime give information on the favored exit channels and on the efficiency of the deactivation process. VP lifetimes of vibrationally excited vdW species are found to vary over a range that exceeds 10 orders of magnitude. We recently demonstrated a link between excited lifetime, amount of energy to be disposed of and the ability of the system (i.e., excited molecule and weakly bound species) to dispose of this energy into molecular rotation.[22] As in the inelastic case there appear to be angular momentum constraints that strongly influence the dissociation and subsequent formation of products. The manner in which molecule and partner species affect the rapidity of dissociation of vdW molecules through AM load reduction is the next topic of discussion.

The series of experiments on $(X)^2\Pi$ OH weakly bound to mono- and polyatomic partners and studied in detail by Lester and co-workers[23-26] vividly illustrate the influence of partner species on speed of dissociation. In this work OH is excited to $(v, n) = (2, 1)$ level of the X-state using an infrared laser and the rotational populations of $v = 1$ are determined by laser-induced fluorescence. Note that in common with general usage, rotational AM in this Π-state radical is denoted by the symbol n_{OH}. Figure 3a presents a diagram of the $v = 1$ and 2 vibrational levels of OH and the rotational levels of $v = 1$ on a relative energy scale. For the purpose of this discussion we restrict consideration to the $j = {}^3/_2$ level of the $^2\Pi$ ground state. It is

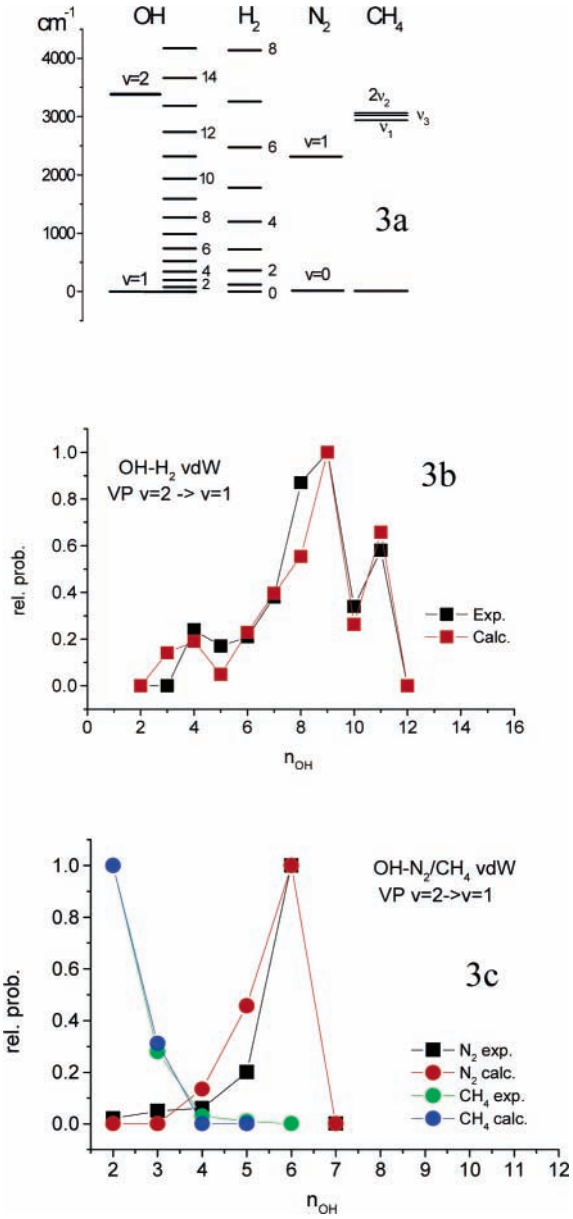

Figure 3. (a) Energy level diagram of the $v = 2$ and $v = 1$ states of $(X)^2\Pi_{1/2}$ OH showing the rotational levels of the lower state. In addition, relevant rotational states of H_2, and vibrational energies of N_2 and CH_4 are displayed. (b) Experimental (black squares) and calculated (red squares) rotational distribution in $v = 1$ of OH following VP of the OH−H_2 vdW molecule. In the calculation, a weighted sum of all energetically possible rotational excitations in H_2 was taken. (c) Experimental and theoretical rotational distribution in $v = 1$ OH following VP of OH−N_2 and OH−CH_4. In the calculations, excitation $v = 1 \rightarrow 2$ for OH−N_2 and excitation of $2v_2$, v_1, and v_3 in OH−CH_4 were assumed. Experimental data taken from refs 24−26.

straightforward to include the $^2\Pi_{1/2}$ level, but this adds unnecessary complexity to the analysis. Here our principal focus is on vdW complexes of (X)OH with Ar, H_2, N_2, and CH_4, which exhibit a wide range of VP lifetimes from $>30 \times 10^{-6}$ s in OH−Ar to 25×10^{-12} s for OH−CH_4.

An initial analysis of this series of vdW molecules was given in a recent publication.[22] Here the $v = 1$ rotational distributions are calculated by assuming deposition of specific fractions of the available energy of dissociation into partner rotation or vibration. The appropriate momentum−AM diagrams are given in ref 22 and are not reproduced here. In the absence of transfer into partner internal motion, the principal channel for VP is predicted[22] to be $n_{OH} \approx 12$ for each of these complexes. (Note that the energy available for conversion into rotation varies slightly with the partner species due to the contribution of the vdW binding energy.) Much lower n_{OH} values are found experimentally[24−26] for H_2, N_2, and CH_4, strongly suggesting the involvement of partner species excitation. The weakly bound partners were chosen by Lester and co-workers[24−26] specifically to illustrate the relative importance of molecular rotation and vibration as acceptor modes for excess energy. Momentum−AM diagrams give a semiquantitative picture of the effect of partner vibration on the expected $v = 1$ rotational peak and these predict[22] shifts to $n_{OH} = 6$ when one quantum of N−N stretch and to $n_{OH} = 2$ when $2v_2$, $1v_3$, and $1v_1$ in CH_4 are excited.

As in the inelastic case, the most probable exit channel is that representing minimum OH rotational change when AM is the dominant constraint with maximum b_n accessed. As seen in examples discussed above, the rotational state change may on some occasions constitute sufficiently large a constraint to be an insurmountable barrier and thus relaxation does not occur despite there being a surfeit of energy to be released. The magnitude of this critical value of rotational AM varies strongly with the species under consideration. In OH the AM change in direct $v = 2 \rightarrow v = 1$ relaxation is relatively modest but OH is a poor converter of impulse into rotation, the principal reason being the energy change associated with each unit of AM change.[7,8] Twelve AM units are readily generated in diatomics such as I_2 and Br_2 with their very small energy requirements and long torque-arms and this is the origin of the very different VP behavior in vdW complexes of halide and hydride diatomics.[22] $v = 2 \rightarrow v = 1$ VP for OH−Ar is a sufficiently constrained process that the diatomic undergoes some 10^7 oscillations before the complex breaks up. This long lifetime is not simply a function of well depth because D_0 for OH−Ar is 93 cm^{-1} and that for OH−CH_4 is 210 cm^{-1}.[23,26] The lifetime of (X)OH−Ar is reported[26] to be $>30 \times 10^{-6}$ s. Thus the probability of generating 13 or 14 AM units is so low as to represent an almost insurmountable barrier to the relaxation of OH by Ar under these low collision energy conditions. $v = 2 \rightarrow v = 0$ VP in OH−Ar would be immeasurably small despite the fact that there is a greater amount of energy available. However, this dissociation might be accomplishable with a suitably chosen vdW partner species as we demonstrate below.

On complexing OH with H_2 new possibilities arise for assisted VP, in this instance through simultaneous excitation of rotational transitions in H_2 as pointed out by Hossenlopp et al.[24] Unlike the $6^1 \rightarrow 0^0$ vibrational deactivation in benzene considered above, the energy gap is sufficiently large that many rotational transitions in H_2 are feasible and the multipeaked appearance of the final distribution[24] (Figure 3b) is evidence that several exit routes exist. In such a situation there will be tradeoff between the increasing probability of VP as the AM load in this species is lightened and diminishing probability of j change in H_2. To identify the principal OH−H_2 dissociation routes, calculations of OH ($v = 1$) rotational distributions were undertaken for all feasible transitions in H_2. The results were weighted to best fit the principal peaks in the experimental distribution and then summed. The resulting data are plotted along with experimental points in Figure 3b. The peak at n_{OH}=11 primarily results from excitation of $0 \rightarrow 2$ and/or $1 \rightarrow 3$ in H_2 whereas the strongest transition at $n_{OH} = 9$ appears mainly to involve $0 \rightarrow 4$ and/or $1 \rightarrow 5$ excitation. The broad structure around $n_{OH} = 4-6$ appears when transitions $0 \rightarrow 6$ and $1 \rightarrow 7$ occur in H_2. The result of these various processes is

a net reduction of the AM load associated with the OH $v = 2 \rightarrow v = 1$ VP and a more efficient dissociation is predicted. The VP lifetime for OH−H_2 is 115×10^{-9} s,[24] more than 2 orders of magnitude faster than in OH−Ar.

That N_2 will be more effective as a vdW partner in the $v = 2 \rightarrow v = 1$ relaxation is readily seen in a momentum−AM diagram,[22] as excess energy may now be deposited into partner species vibration. The energy levels of N_2 (Figure 3a) show that 2330 cm^{-1} of energy may be disposed of in this fashion, leading to a reduction in the AM load such that peak $n_{OH} = 6$. The experimental data of Marshall et al.,[25] reproduced in Figure 3c, demonstrate this qualitative guide to be quite accurate and quantitative calculations in which 2330 cm^{-1} has been removed from the available dissociation energy confirm the interpretation by reproducing the experimental distribution with quite reasonable accuracy. The VP lifetime of this species is 30×10^{-9} s,[25] i.e., 1000-fold faster than for OH−Ar.

The correlation between reduced AM load and faster VP is dramatically illustrated by the VP behavior of OH−CH_4.[26] Some of the high-lying vibrational states of CH_4 are shown in Figure 3a from which it is evident that a substantial fraction of the energy available on VP may be disposed into partner vibration by involving these modes as energy acceptors. The CH_4 levels shown are part of a polyad in the region around 3000 cm^{-1} and should one of these be excited on dissociation, the AM load would be very much reduced. Thus, for example, the excitation of two quanta of the ν_2 mode shifts the principal dissociation channel to $n_{OH} = 2$ and when ν_1 and ν_3 are acceptor modes $n_{OH} = 3$ may also be populated. Quantitative calculations that include these collaborative excitations exhibit an OH rotational peak at $n_{OH} = 2$, in good agreement with experiment (Figure 3c). Note that the $n_{OH} = 1$ population could not be measured because of experimental difficulties[26] though calculation predicts this to have significant probability. The VP lifetime was measured at 25×10^{-12} s, 6 orders of magnitude faster than the same process in OH−Ar.

The trends described in the series of OH vdW complexes with Ar, H_2, N_2, and CH_4 follow those observed in the vibrational deactivation of benzene in low-energy collisions and Li_2−Xe undergoing high-energy encounters. The most favored dissociation channel is that requiring the lowest AM change consistent with dominant AM constraint when maximum available torque-arm is accessed. The VP data establish a quantitative link between AM load and speed of dissociation and, like the VRT results, demonstrate that there are constraints on exit channel processes that on occasions may be too great for the system to overcome and thus they constitute a form of barrier. The origin of this restriction is the exponential-like fall of transition probability as the AM change increases and thus there are processes for which this probability is simply too low. The very slow VP rate in OH−Ar is indicative of a system only just able to meet the AM consequences of this energy release. However, the VRT results for $6^1 \rightarrow 0^0$ relaxation in benzene[15−17] and data for $2 \rightarrow 1$ vibrational predissociation in OH−X vdW molecules[23−26] suggest practical means of overcoming exit channel constraints. These involve AM load reduction by utilizing acceptor modes in partner species and may take the form of partner rotation and/or vibration. The increase in rate of dissociation, or probability of relaxation, by a suitably chosen partner species has many of the features associated with catalysis and this is an aspect we return to in a later section.

3. Exothermic Chemical Reactions

In extending the above analysis to reactive collisions, one must first note that even the simplest of reactions is considerably more complex than the inelastic and dissociative events considered thus far. A model of this event must, in reasonably transparent fashion, incorporate such factors as (i) change of coordinate frame during the collision as nuclei exchange, (ii) disposal of energy and the change of energy "reference point" on reaction and (iii) the formation of rotationally and vibrationally excited products. A feature of most models of chemical reaction is that in their evolution from kinetic theory, through transition state theory, to quantum reactive scattering[27] they have become less rather than more transparent. In a series of publications[28,29] we have described an extension of the AM model of inelastic collisions to the reactive domain with the aim of recovering some of the insights available from early models without greatly sacrificing accuracy. This momentum-change approach shares elements in common with the "classical kinematic" model of Elsum and Gordon[30] and appears to be an excellent predictor of product vib-rotational distributions, reproducing experimental reaction cross-sections with very reasonable accuracy.[28,29]

The key elements of this model are as follows.[29] Orbital AM of relative motion is converted to product rotational AM in a highly localized region, the *critical configuration*. In the reaction $A + BC \rightarrow AB + C$ the critical configuration is reached when atom A makes contact with an ellipsoid shape at which momentum is exchanged. For a homonuclear reactant this ellipsoid has dimensions[28] $a = 2R_B + R_A$ and $b = R_A + R_B$, where a and b are the semimajor and semiminor axes, respectively, and R_X represents an atomic radius. Depending on the angle at which the reactants approach, the critical configuration may be achieved with the AB bond elongated or compressed relative to its equilibrium length, each of these situations representing vibrational excitation of the product species. This increased energy is readily quantified and product vibrational states identified.[28] Product rotational state assignment is made via the expression[4,30] $j_f = l_i \sin^2 \beta + j_i \cos^2 \beta + d \cos^2 \beta$ where subscripts i and f refer to reactant and product angular momenta, respectively. The parameter β relates distances in the product coordinate frame to those in the reactant frame. Expressions for d are readily found in the works referenced.[4,28,30] Reaction enthalpy, in this model, is converted to relative velocity of the reactant pair and added to (exothermic reaction) or subtracted from (endothermic reaction) the collision velocity. This simple approach, justified elsewhere,[28] is found to be quite effective in chemical reactions and in inelastic processes when, e.g., one of the species is electronically excited.

Thus a transparent model exists with which to analyze elementary chemical reactions and here we use this in conjunction with experimental data to identify constraints that might inhibit the formation of products in reactive exit channels. However, reactions in which fully resolved data have been obtained are sparse and unambiguous evidence of the kind found in inelastic and dissociative processes is more difficult to identify. In reactions for which state-to-state data exist, quite evidently constraints on the formation of products have been overcome and thus our criteria for the existence of any form of hindrance to the formation of products must primarily focus on the *efficiency* of the process as measured by reaction cross-section or rate constant. Other relevant observables include, as in the case of inelastic and dissociative processes, the nature of preferred product channels in the nascent species and also the fate of these species as the products proceed to equilibration.

3.1. Graphical Representation. The underlying physical principles of the model may once again be displayed in velocity−AM plots, provided the key features of reactive encounters are incorporated. Thus the product (v, j) states are those of the new species and energy change calculations must reflect this. Product rovibrational states are displaced down or up the energy scale according to whether the reaction is exo- or endothermic, respectively. The reaction $F + I_2 \rightarrow IF + I$ is chosen as illustrative in view of the extensive data available on this system.[32] Figure 4a is an energy level diagram of initial and final ($v_{IF} = 9$, 11, 17) vj states. This exothermic reaction has $\Delta D_0 = -1.226$ eV, where ΔD_0 is the dissociation energy difference. The energy zero[28] is given by the available energy (enthalpy + collision energy) corrected for the experimentally determined fraction available for internal excitation. Note that a reasonable approximation to the fraction that is disposed as recoil may be calculated from the kinematic equations[4] though here we use experimental values throughout.

Relative velocity (v_r)−product rotational state (j_{IF}) diagrams represent disposal of initial energy into product rotation *once a given vibrational channel has opened*. Thus there will be a unique plot for each v_f level, with the $j_{IF} = 0$ channel velocity in each case that which opens the relevant vibrational channel. The energy available for rotation decreases as that required to open the vibrational level increases, illustrated in Figure 4b for $v_{IF} = 9$, 11, and 17. The backward-arching curves in Figure 4b reflect the diminishing energy gap as j_{IF} increases until the reactant zero point is reached, beyond which the gap begins to increase. The range of j_{IF} values accessible for $v = 11$ is less than that for $v = 9$ and is even smaller for $v = 17$. The reaction liberates a pulse of energy, the greater part of this and velocity of relative motion (in this $\cos^2 \beta \approx 0$ case) being disposed into product vibration and rotation. In the conversion of reactant orbital AM to product rotation, $j_{IF} \approx l_{A-BC}$, where l_{A-BC} is the orbital AM generated at the critical configuration by atom A about diatomic BC. The maximum value of initial orbital AM (l_{max}) is readily calculated and will vary with the product vibrational state. In Figure 4b the horizontal lines represent $l_{max} = 143$, 133, and 68 for $v = 9$, 11, and 17, respectively, and the vertical lines show the maximum velocity available for conversion to orbital AM for that v_f state.

Note that the limiting condition of the model requires that orbital AM formed initially at the critical configuration be converted to product rotation with no recoil orbital AM. Population of the $j_{IF} < j_{max}$ states of $v = 9$ and 11 occurs through trajectories in which $l < l_{max}$, i.e., torque-arm (R_{A-BC})[28] values that are less than the maximum obtainable at the critical configuration. Thus for the $j_{IF} = 0$ channel of each v_{IF} level, R_{A-BC} is zero and the impulse is converted principally into product molecule vibration. The reactive analogue to the *A*-plots of Figures 1b and 2b would be a line joining j_{max} at $v_r = 0$ (in Figure 4b) to $j = 0$ at v_r^{max} with the implied interpretation that v_r represents a velocity "defect", i.e., that unavailable to be converted to product rotation. We elaborate on this approach in a future publication[31] in which we demonstrate those velocities lying *between* the *A*- and the *E*-plot are those allowed by energy and AM conservation.

Figure 4b plots the state-to-state channel opening conditions for rotational levels of $v = 9$, 11, and 17 assuming all energy available for internal excitation becomes product rotation within that vibrational state; i.e., it is the energy conservation condition for each individual level. It is evident from these plots that channels close to the maximum available will be especially favored because they are open for a large fraction of available velocities. The figures give a qualitative indication of the shape of final rotational distributions because for each j_{IF} channel the transition probability will be related to the number of allowed trajectories for that channel. The overall rotational distributions

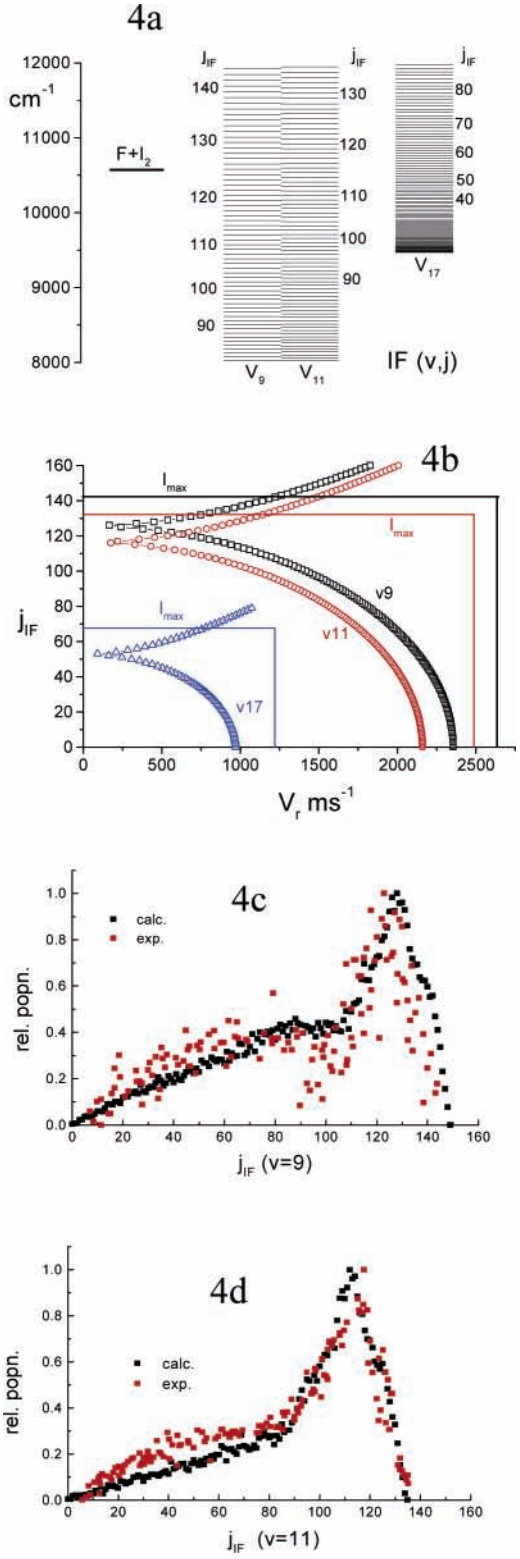

Figure 4. (a) Diagram showing relative energies of reactants and products in the $F + I_2 \rightarrow IF + I$ reaction. Reactants are assumed to be in their lowest (v, j) levels and the rotational levels of $v = 9$, 11, and 17 of IF are shown. (b) Velocity−AM diagram for $v = 9$, 11, and 17. See text for further description. (c), (d) Experimental (red squares) and calculated (black squares) rotational distributions for $v = 9$ and 11 of product IF. Experimental data from Girard et al.[32]

are predicted to be similar in shape for two of the cases considered. Principal peaks are expected at $j_{IF} = 125$ for $v = 9$, 116 for $v = 11$, and 69 for $v = 17$. Each will have a "tail" of probabilities down to low j_{IF} values. Figure 4c shows experimental rotational distributions[32] for two vibrational states of IF together with distributions calculated using the method described above.[28] Experimental data are characterized by a principal peak at high j_{IF} and a longer tail to low j values. The calculations reproduce the overall shape and peak positions of most measured vj distributions well, though there are small discrepancies at higher vj where the IF spectroscopic constants are less well established. These results together with other evidence[28,29] indicate that the method is robust and that the underlying physical principles provide a satisfactory representation of the dynamical processes involved.

What do these and related state-to-state data tell us about the most likely exit channels from the transition state? First, it is evident that the transition from reactants to products is initially a near-energy-resonant process in which, for a given vibrational level, the preferred exit route involves minimum AM *change* (in the $l_{A-BC} \rightarrow j_{IF}$) process consistent with energy conservation. As in the inelastic and dissociative cases the most probable transition is that for which the greatest number of velocities, and hence collision trajectories can contribute to population of that channel. Relaxation to lower levels of the product species would follow in a typical chemical environment as further collisions take place. Second, the deposition of energy into product vibration reduces the AM that must be generated within that vibrational state. There is some disagreement concerning the overall shape of the product IF vibrational state distribution, but the data of Girard et al.[32] and those reported by Trikl and Wanner[33] both indicate that high vibrational levels are preferred. Third, this quite clearly is a facile reaction with measured cross-section[34] around 70 Å^2. Two factors are noted in conjunction with this last observation, the first of these being the large number of potential product states in the critical near-resonant region and the second, the efficiency of IF as a converter of impulse into molecular rotation, a property that is the result of this molecule's long bond length and small rotational constant.[7,8]

In marked contrast to the above example is the reaction (7P)-Cs + $H_2 \rightarrow$ CsH + H studied by L'Hermite et al.[35] Here, this reaction, which is highly endothermic for reactants in their ground states, becomes just exothermic (by 13 cm^{-1}) when the Cs atom is excited to the $7P_{1/2}$ state. Data at experimental collision energy 0.09 eV are considered here and the kinematics of this light atom exchange process ($\cos^2 \beta \approx 0.5$) dictate that a substantial fraction of initial velocity be converted to orbital AM of the products. L'Hermite et al. report that 0.063 eV is disposed as product kinetic energy[35] and the reactant energy "zero" shown in Figure 5a, used in the calculations for Figure 5b, incorporates this experimental value. The overall reaction cross-section is reported to be 4.2 Å^2 at 0.09 eV, and the authors[35] suggest that this reaction proceeds via the harpoon mechanism, explaining the low cross-section as the result of a quenching process that involves one or more of the many intersecting surfaces of a very complex PES.

Parts a and b of Figure 5 indicate that near-resonant transitions to $j_{CsH} \approx 10$ will be favored with the maximum observable $j = 16$. Thus a broad distribution centered close to $j = 10$ would be anticipated with populations less peaked to high j values than in the case of IF from F + I_2 where the near-resonant j values are close to j_{max}. The experimental results support this qualitative analysis and the j distributions in the $v = 0$ level are accurately reproduced in quantitative calculations both for 0.09 and for

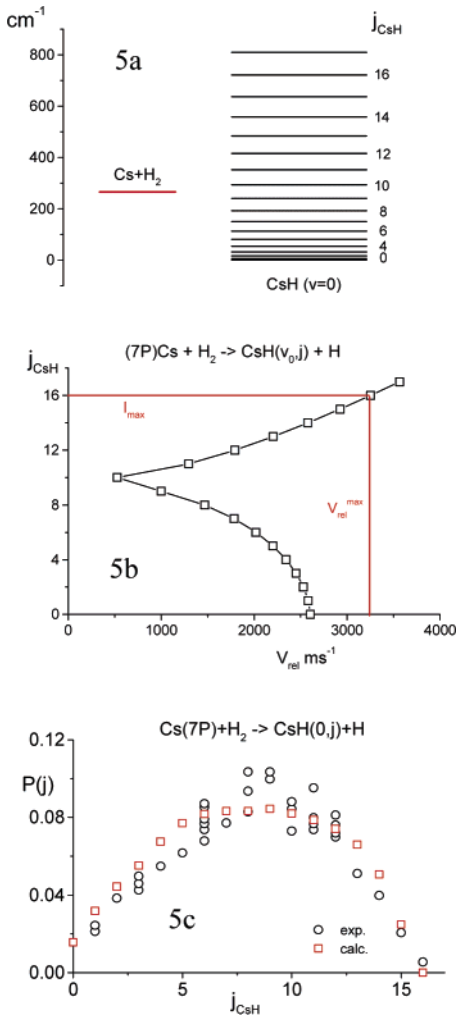

Figure 5. As for Figure 4 but now the diagrams refer to the reaction (7P)Cs + $H_2 \rightarrow$ CsH + H. In (c) black circles represent experimental data (from L'Hermite et al.[35]) and red squares calculated points.

0.045 eV collision energy[29] displayed for the former energy in Figure 5c. Thus the transition from reactants to products follows initial pathways very similar to those described in F + I_2. Now, however, only CsH (0, j) channels are open, and as a result, the number of accessible product states is very small. Only a small fraction of initial trajectories will meet the energy and momentum conditions that lead to the opening of a product quantum state, and this is a significant difference between the Cs + H_2 reaction and that yielding IF from F + I_2. However, like IF, CsH is a reasonably efficient converter of reactant orbital AM to product rotation because it has a long bond length (2.5 Å) and relatively small rotational constant.

We further develop the theme that probability of reaction might be related to the factors discussed above, i.e., (i) the efficiency of the product diatomic in converting reactant orbital AM into molecular rotation and (ii) the number of accessible product states. Two further classes of reaction are considered, one characterized by low probability with cross-sections ~1−3 Å^2 and the other a set of facile reactions with cross-sections ~100−200 Å^2. Examples of the first category are the H + HX $\rightarrow$ H_2 + X reactions (X = halogen) studied by Aker et al.[36,37] and by Kliner et al.[38] These reactions are initiated by high-velocity H-atoms from photolysis of the halide and the enthalpy contribution to overall reaction energetics varies from strongly exothermic (X = I) to nearly thermoneutral (X = Cl) with X = Br intermediate between these two. As a result, a number of

(v, j) channels of product H_2 that are accessible though these product states will be well separated in the near-resonant region. Shown on an energy level diagram this system would resemble the plot of Figure 5a but accessible final rovibronic states would be considerably less dense than displayed in that figure. Thus the number of potential product quantum states is very limited and stringent energy and momentum criteria must be met by the reactants to access these product states. Additionally, H_2 is a poor converter of orbital-to-rotational AM[6−8] because it possesses a particularly short torque-arm. These factors indicate low reaction probability for a given reactant trajectory and the characteristically low cross-sections for these reactions bear this out.[36−38] A further difficulty in these reactions may arise from the production of highly excited H_2. This species is particularly difficult to relax once in a high-(v, j) state[39] and thus the prospect of a reverse reaction is enhanced.

At the other extreme are the alkali atom + dihalogen reactions extensively studied by Herschbach and co-workers.[40] These have very large cross-sections: 220 Å^2 for production of KBr from K + Br_2 and 410 Å^2 for RbBr from Rb + Br_2, for example.[40] The magnitude of these cross-sections is usually explained by invoking the harpoon mechanism,[41,42] though, in the light of the above discussion, an alternative interpretation of the rate of these highly exothermic reactions ($\Delta D_0 \sim 150-200$ kJ mol^{-1}) might be considered. The reaction K + $Br_2 \rightarrow$ KBr + Br is typical of a wide range of alkali−halogen reactions. KBr has a very low vibrational frequency (213 cm^{-1}) with rotational constant 0.081 22 cm^{-1} [43] so that near-energy-resonant transitions from the reactants to product KBr may take place to one of more than 100 vibrational levels in each of which rotational j_f values up to 400 are within the accessible energy range. The energy level diagram for this reaction would have a density of states considerably greater than shown in Figure 4a for example. The number of product states in the critical near-resonance region will be very high indeed and thus a very high fraction of reactant trajectories will meet the energy and momentum criteria needed for a (v, j) channel of KBr to open. Furthermore, with its small rotational constant and bond length of 2.82 Å this molecule will be a very efficient converter of impulse into molecular rotation. The molecular beam study of this reaction by Birely et al.,[40] though lacking state-to-state resolution, ascertained that the products are indeed formed initially in very high-v and -j states as would be predicted from the analysis outlined above.

To summarize the experimental data on preferred exit channels from the transition state in reactive collisions, it is evident that there are striking similarities to related processes of deactivation by inelastic collisions or by dissociation. The initial step consists of a near-resonant transition to a product state, the most probable channels being those most strongly allowed under constraints provided by AM and energy conservation. Products will generally be formed in excited states, often in very high-lying vibrational and rotational levels. Equilibration of these may be fast though this will depend on the nature of the products and bath species. The diatomic hydrides in high-(v, j) states are known to be particularly slow to equilibrate and products such as H_2, OH, HF, HCl, etc. may remain excited through many collisions as a result of quasi-resonant vibration−rotation transfer,[39,44] thus increasing the probability of a reverse reaction. The disposal of some fraction of available energy into product *vibration* generally will increase the transition probability by reducing the AM load, as found in inelastic and dissociative processes. However, there may be competition between this and the energy and momentum requirements for opening each vibrational state. The overall rate of transition may be quantifiable in terms of two principal elements, one of which expresses the efficiency of conversion of orbital-to-rotational AM and the other the number of accessible product states.

4. Summary and Conclusions

Close examination of experimental data from a wide range of relaxation processes in molecules activated by a variety of methods reveals a number of significant common elements. In each process the preferred first step in the deactivation consists of a transition to the final v, j state that represents the minimum AM change for which the maximum number of trajectories is allowed. In the relaxation of activated species by nonreactive events, an equivalent statement would be that the initial step involves a transition of minimum Δj for which AM is the dominant constraint when maximum available torque-arm is used.

This initial transition is often a near-resonant process in energy terms, though it may involve the generation of a substantial amount of rotational angular momentum. Analysis of a wide range of data and, significantly, of processes that are not observed leads us to suggest that constraints can strongly influence the formation of products in the deactivation of energy-rich molecules both in collision-induced relaxation and in dissociation. These constraints are associated with the amount of angular momentum that must be generated in the deactivation, and the AM load will generally increase as the energy gap between initial and final states increases. The probability of generating rotational AM falls very rapidly as the magnitude of Δj increases and this effectively limits the size of the (nominal) energy gap that may be bridged by a given molecule−collision partner pair. Thus, whatever the level of excitation contained within a species, there is a limit to the amount of energy that may be released in a single collision event. Often, significant amounts of excitation remain within molecules following collision for reasons that appear to be related solely to the capacity of the system to generate the necessary amount of rotational AM. In such a case the constraint is of sufficient magnitude that it constitutes a barrier to the deactivation process. We note that the temperature dependence of angular momentum constraints of the kind described above is expected to be Arrhenius-like for just the reasons described in the Introduction.

Experiment indicates how exit channel constraints on the de-excitation of molecules by inelastic and dissociative processes may best be overcome. Deposition of some fraction of the available energy into rotation or vibration within the partner species reduces the AM load the excited molecule must generate in the first step of the deactivation process. Reduction of the rotational AM requirements in a deactivation process results in higher yield of the relaxed products and/or a shorter dissociative lifetime. The gain in dissociation rate by this mechanism may be spectacular, as demonstrated by Lester and co-workers.[23−26] State-resolved reactive collisions appear to be controlled by closely related forces so that the principle of minimum AM change (orbital-to-rotational) within the constraints provided by energy conservation leads to a set of principal reaction pathways that consist of near-energy-resonant transitions as the initial step. Thus, by analogy to the inelastic and dissociative cases, we suggest that deposition of available energy into product vibration would lead to enhanced reaction rate. There is experimental evidence that transitions to high product vibrational levels are generally more probable than those to low-v states. However, the threshold velocity required to open a vibrational channel

also constitutes a constraint and this effect will compete with diminished AM load resulting from the reduction in effective energy gap.

Thus, on the basis of the foregoing, it might be possible to devise strategies to overcome constraining factors in the exit channel and thus obtain a significant increase in the rates of chemical reactions. The presence of a product species having vibrational modes capable of absorbing a substantial fraction of the available energy is likely to be rate enhancing. This may in some instances be a mode-selective process in view of the high degree of selectivity found in the vibrational relaxation of excited polyatomic molecules[13,14] and simple energy resonance may not be sufficient in complex species. The transition from reactant to products should be enhanced by product species that readily convert impulse into rotation.[6,8] Products with a high density of states in near-resonance with the available reactant energy are likely to be advantageous because they increase the probability a given reactant trajectory will meet the energy and momentum criteria needed to open a product channel. If such exit channel constraint reduction strategies prove to be successful, new light may be thrown on the mechanism of catalysis, in particular the manner in which the process operates and how it may be optimized. Thus in seeking methods of accelerating chemical reactions, it may be more profitable to focus on efficient means of disposing of the available energy *post-transition state* rather than on mode-selective methods of accessing the transition state.

As noted above, there are product species that are best avoided in gas phase reactions when the objective is to achieve highest yield. Molecules such as OH, HF, HCl, etc. have inherently low densities of rovibronic states and are relatively poor at converting momentum. Furthermore, once in high-*j* states they are not readily deactivated and may exchange rotational for vibrational energy and vice versa, remaining highly excited throughout many thousands of collisions[44] and thereby enhancing the possibility of a reverse reaction. We have drawn attention to a possible connection between the reaction cross-section and the combined effect of (i) ease with which orbital AM of reactants is converted to rotational AM of products and (ii) the number of product rovibronic states accessible, particularly those in the critical near-resonant region. An approach to rates of elementary reactions through this route might provide a simpler and more visual link from microscopic to macroscopic observables.

Acknowledgment. M.A.O. thanks the Royal Society for a University Research Fellowship. Helpful discussions with Dr. G. A. Lawless and Professors G. J. Leigh, M. F. Lappert and J. F. Nixon, W. D. Lawrance, and S. D. Bosanac are acknowledged. Prof. K. McKendrick first drew the authors' attention to the absence of satisfactory explanation for energy-releasing processes that fail to occur.

References and Notes

(1) Arrhenius, S. *Z. Phys. Chem*. **1899**, *4*, 226.
(2) See for example: Laidler, K. J. *Chemical Kinetics*, 3rd ed.; Harper & Row: New York, 1987 (see also other works by this author).
(3) Marcelin, R. *Compt. Rend.* **1914**, *158*, 116, 407.
(4) Levine, R. D.; Bernstein, R. B *Molecular Reaction Dynamics and Chemical Reactivity*; Oxford University Press: Oxford, NY, 1987.
(5) See for example Sirkin, E. R.; Pimentel, G. C. *J. Chem. Phys*. **1981**, *75*, 604−612.
(6) McCaffery, A. J.; AlWahabi, Z. T.; Osborne, M. A.; Williams, C. J. *J. Chem. Phys*. **1993**, *98*, 4586−4602. Osborne, M. A.; McCaffery, A. J. *J. Chem. Phys*. **1994**, *101*, 5604−5614.
(7) Marsh, R. J.; McCaffery, A. J. *J. Phys. B At. Mol. Opt. Phys*. **2003**, *36*, 1363−1382.
(8) McCaffery, A. J. *Phys. Chem. Chem. Phys*. **2004**, *6*, 1637−1657.
(9) Magill, P. D.; Scott, T. P.; Smith, N.; Pritchard, D. E. *J. Chem. Phys*. **1989**, *90*, 7195−7205. Stewart, B.; Magill, P. D.; Pritchard, D. E. *J. Phys. Chem. A* **2000**, *104*, 10565−10575.
(10) McKendrick, K. Private communication
(11) Besley, N. A.; McCaffery, A. J.; Osborne, M. A.; Rawi, Z. *J. Phys. B At. Mol. Opt. Phys*. **1998**, *31*, 4267−4282.
(12) Polanyi, J. C.; Woodall, K. B. *J. Chem. Phys*. 1972, *56*, 1563−1572. Brunner, T. A.; Pritchard, D. E. *Adv. Chem. Phys.* **1982**, *50*, 589−611.
(13) Flynn, G. W.; Parmenter, C. S.; Wodtke, A. M. *J. Phys. Chem*. **1996**, *100*, 12817−12838.
(14) Rice, S. A. *J. Phys. Chem*. **1986**, *90*, 3063−3072.
(15) Waclawik, E. R.; Lawrance, W. D. *J. Chem. Phys*. **1995**, *102*, 2780−2791.
(16) Waclawik, E. R.; Lawrance, W. D. *J. Chem. Phys*. **1998**, *109*, 5921−5930.
(17) Waclawik, E. R.; Lawrance, W. D. *J. Phys. Chem. A* **2004**, *107*, 10507−10513.
(18) McCaffery, A. J.; Osborne, M. A.; Marsh, R. J.; Lawrance, W. D.; Waclawik, E. R. *J. Chem. Phys*. **2004**, *121*, 169−181.
(19) Schinke, R *Photodissociation Dynamics*; Cambridge University Press: Cambridge; 1993.
(20) Levy, D. H. *Annu. Rev. Phys. Chem*. **1980**, *31*, 197−217; *Adv. Chem. Phys*. **1981**, *47*, 323−346.
(21) Lester, M. I. *Adv. Chem. Phys*. **1996**, *96*, 51−84.
(22) McCaffery, A. J.; Marsh, R. J. *J. Chem. Phys*. **2003**, *117*, 9275−9285.
(23) Berry, M. T.; Brustein, M. R.; Lester, M. I. *J. Chem. Phys*. **1989**, *90*, 5878−5879.
(24) Hossenlopp, J. M.; Anderson, D. T.; Todd, M. W.; Lester, M. I. *J. Chem. Phys*. **1998**, *109*, 10707−10718.
(25) Marshall, M. D.; Pond, B. V.; Hopman, S. M.; Lester, M. I. *J. Chem. Phys*. **2001**, *114*, 7001−7012.
(26) Wheeler, M. D.; Tsiuris, T.; Lester, M. I.; Lendvay, G. *J. Chem. Phys*. **2000**, *112*, 6590−6602.
(27) Miller, W. H. *Faraday Discuss. Chem. Soc*. **1998**, *110*, 1−21.
(28) Marsh, R. J.; McCaffery, A. J.; Osborne, M. A. *J. Phys. Chem*. **2003**, *107*, 9511−9521.
(29) Truhins, K.; Marsh, R. J.; McCaffery, A. J.; Whiteley, T. W. J. *J. Chem. Phys*. **2000**, *112*, 5281−5291. McCaffery, A. J.; Truhins, K.; Whiteley, T. W. J. *J. Phys. B At. Mol. Opt. Phys.* **1998**, *31*, 2023−2043.
(30) Elsum, I. R.; Gordon, R. G. *J. Chem. Phys*. **1982**, *76*, 3009−3018.
(31) McCaffery, A. J.; Osborne, M. A. Manuscript in preparation.
(32) Girard, B.; Billy, N.; Gouedard, G.; Vigue, J. *J. Chem. Phys*. **1991**, *95*, 4056−4069. Girard, B.; Billy, N.; Gouedard, G.; Vigue, J. *Faraday Discuss. Chem. Soc*. **1987**, *84*, 65−73.
(33) Trikl, T.; Wanner, J. *J. Chem. Phys*. **1983**, *78*, 6091−6101.
(34) Appleman, E. H.; Clyne, M. A. A. *J. Chem. Soc., Faraday Trans*. **1975**, *1*, 2072−2084.
(35) L'Hermite, G. M.; Rahmat, G.; Vetter, R. *J. Chem. Phys*. **1990**, *93*, 434−444; **1991**, *95*, 3347−3360.
(36) Aker, P. M.; Germann, G. J.; Valentini, J. J. *J. Chem. Phys*. **1989**, *90*, 4795−4808.
(37) Aker, P. M.; Germann, G. J.; Valentini, J. J. *J. Chem. Phys.* **1992**, *96*, 2756−2761.
(38) Kliner, D. A. V.; Rinnen, K. D.; Buntine, M. A.; Adelman, D. E.; Zare, R. N. *J. Chem. Phys*. **1991**, *95*, 1663−1670.
(39) Clare, S.; McCaffery, A. J. *J. Phys. B At. Mol. Opt. Phys*. **2001**, *33*, 1121−1134.
(40) Birely, J. H.; Herm, R. R.; Wilson, K. R.; Herschbach, D. R. *J. Chem. Phys.* **1967**, *47*, 993−1004.
(41) Polanyi, M. *Atomic Reactions*; Williams and Norgate: London, 1932.
(42) Magee, J. L. *J. Chem. Phys*. **1949**, *8*, 3−12.
(43) Huber, K. P.; Herzberg, G. *Molecular Spectra and Molecular Structure IV. Constants of Diatomic* Molecules; Van Nostrand Reinhold: New York, 1979.
(44) Marsh, R. J.; McCaffery, A. J. *J. Chem. Phys*. **2002**, *117*, 503−506.